Scattering from a Metamaterial Hemispherical Boss on an Infinite Plane

A.-K. Hamid[1] and F.R. Cooray*,[2]

[1]*Department of Electrical and Computer Engineering, University of Sharjah, Sharjah, United Arab Emirates;* [2]*CSIRO ICT Centre, P.O. Box 76, Epping, NSW 1710, Australia*

Abstract: An exact solution is presented to the problem of scattering of a plane electromagnetic wave from a metamaterial hemispherical boss located on an infinite conducting plane, using the method separation of variables. The formulation is based on an image technique, where the original problem is replaced by that of scattering of two plane waves by the corresponding sphere in the absence of the infinite plane. The solution is obtained by expressing all the electromagnetic fields associated with the problem in terms of vector spherical wave functions, and then imposing the appropriate boundary conditions. Numerical results are presented as normalized backscattering cross sections for hemispherical bosses of different sizes and types, for both transverse electric and transverse magnetic polarizations of the incident wave.

INTRODUCTION

Analyses pertaining to the scattering of a plane wave from a semi-cylindrical boss, a hemispherical boss [1-4] and a hemispheroidal boss [5], and scattering of a Gaussian beam from a hemispherical boss [6] have been presented in the literature, when the boss is located on an infinite conducting plane. These analyses have been carried out using the method of separation of variables and the image theory, and serve as benchmarks for validating solutions obtained using other approximate and/or numerical methods. The main motivation for these solutions has been the ability to model a rough surface using a distribution of such bosses [1]. All of the bosses considered in the above mentioned analyses have been either perfectly conducting or non-lossy dielectric. In this paper, we analyze the scattering of a plane electromagnetic wave from a metamaterial hemispherical boss located on an infinite perfectly conducting plane, also using the method of separation of variables.

Since recently, there has been a lot of interest in metamaterials, as a result of the peculiar properties associated with these materials [7-9]. A metamaterial is categorized according to whether its permittivity and permeability are positive or negative. If permittivity and permeability are both positive, it is known as a double positive (DPS) metamaterial, and if both of them are negative it is known as a double negative (DNG) metamaterial. If the permittivity is negative and the permeability is positive the material is called an epsilon negative (ENG) metamaterial and if the permittivity is positive and the permeability is negative, the material is called a mu negative (MNG) metamaterial [10].

In this paper, we will be considering the scattering effects of hemispherical bosses made up of all four kinds of metamaterials, when they are illuminated by a plane wave.

FORMULATION OF THE PROBLEM

Consider a monochromatic plane electromagnetic wave incident at an arbitrary angle on a hemispherical boss made up of a metamaterial substance of permittivity ε_t and permeability μ_t, located on an infinite perfectly conducting plane. The center of the boss of radius a is assumed to be located at the origin O of a Cartesian coordinate system as shown in Fig. (**1**), so that the infinite conducting plane is the x-y plane. The medium in which the boss is located is assumed to be free space with permittivity ε_0 and permeability μ_0. Without any loss of generality, the $y = 0$ plane can be assumed to be the plane of incidence of the arbitrary polarized plane wave, with the incident propagation vector $\boldsymbol{k}_i$ making an angle θ_i with the z axis. A time dependence of $\exp(j\omega t)$ is assumed throughout, but suppressed for convenience.

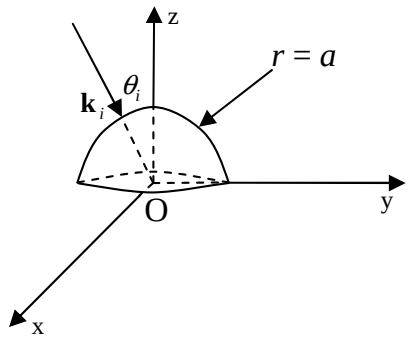

Fig. (1). Geometry of the hemispherical boss located on the infinite plane.

If image theory is used, then the solution to the above problem shown in Fig. (**1**) can be obtained by solving the alternative problem of scattering of two plane waves by the corresponding full sphere, in the absence of the infinite perfectly conducting plane, as shown in Fig. (**2**).

One of these plane waves is the original incident wave while the other is its image on the infinite conducting plane, in the absence of the boss. The arbitrarily polarized incident

*Address correspondence to this author at the CSIRO ICT Centre, P.O. Box 76, Epping, NSW 1710, Australia; E-mail: Francis.Cooray@csiro.au

1874-1290/08

wave can be resolved into transverse electric (TE) and transverse magnetic (TM) components.

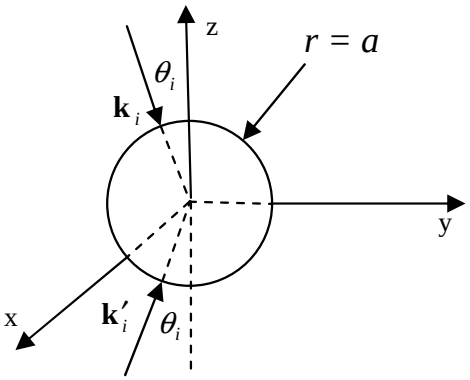

Fig. (2). Geometry of the equivalent problem.

EXPANDING THE FIELDS IN TERMS OF VECTOR WAVE FUNCTIONS (TE CASE)

For TE polarization, the electric field of the original incident wave can be written as

$$\mathbf{E}_i = \hat{\mathbf{y}}\, e^{-j\mathbf{k}_i\cdot\mathbf{r}} \tag{1}$$

where $\hat{\mathbf{y}}$ is the unit vector along the positive y axis, and $\mathbf{k}_i$ is the incident propagation vector given by

$$\mathbf{k}_i = -k_0(\sin\theta_i\hat{\mathbf{x}} + \cos\theta_i\hat{\mathbf{z}}) \tag{2}$$

in which $k_0 = \omega\sqrt{\mu_0\varepsilon_0}$ is the wavenumber in free space. The electric field corresponding to the image of this incident wave on the infinite conducting plane in the absence of the boss, is given by

$$\mathbf{E}_i' = -\hat{\mathbf{y}}\, e^{-j\mathbf{k}_i'\cdot\mathbf{r}} \tag{3}$$

with

$$\mathbf{k}_i' = -k_0[\sin(\pi-\theta_i)\hat{\mathbf{x}} + \cos(\pi-\theta_i)\hat{\mathbf{z}}]. \tag{4}$$

The image wave is the corresponding plane wave reflected by the infinite perfectly conducting plane in the absence of the boss, such that the tangential components of $\mathbf{E}_i + \mathbf{E}_i'$ are zero on this plane.

The electric field of the original incident wave can be expanded in terms of vector spherical wave functions as [11, 12]

$$\mathbf{E}_i = \sum_{m=0}^{\infty}\sum_{n=m}^{\infty}[c_{mn}\mathbf{M}_{emn}^{r(1)}(k_0,\mathbf{r}) + d_{mn}\mathbf{N}_{omn}^{r(1)}(k_0,\mathbf{r})] \tag{5}$$

where $\mathbf{M}_{emn}^{r(1)}$ and $\mathbf{N}_{omn}^{r(1)}$ are the vector spherical wave functions given in the Appendix, $\mathbf{r}$ denotes the spherical coordinate triad (r,θ,ϕ), and c_{mn}, d_{mn} are the incident field expansion coefficients given by

$$c_{mn} = -(2-\delta_{0m})\, j^n \frac{(2n+1)(n-m)!}{n(n+1)(n+m)!}\frac{dP_n^m(\cos\theta_i)}{d\theta_i} \tag{6}$$

$$d_{mn} = 2j^{n-1}\frac{(2n+1)(n-m)!}{n(n+1)(n+m)!}\frac{mP_n^m(\cos\theta_i)}{\sin\theta_i} \tag{7}$$

where δ_{0m} is the Kronecker delta function and $P_n^m(u)$ is the associated Legendre function of the first kind of order m, degree n and argument u.

The expansion of the magnetic field corresponding to the original incident wave in terms of vector spherical wave functions can be obtained from that of the original incident electric field by using Maxwell's equations as

$$\mathbf{H}_i = \frac{j}{\eta_0}\sum_{m=0}^{\infty}\sum_{n=m}^{\infty}[c_{mn}\mathbf{N}_{emn}^{r(1)}(k_0,\mathbf{r}) + d_{mn}\mathbf{M}_{omn}^{r(1)}(k_0,\mathbf{r})] \tag{8}$$

where $\eta_0 = \sqrt{\mu_0/\varepsilon_0}$ is the free space wave impedance. The unknown scattered and transmitted electric and magnetic fields due to $\mathbf{E}_i$ and $\mathbf{H}_i$ can similarly be expanded in terms of vector spherical wave functions as

$$\mathbf{E}_s = \sum_{m=0}^{\infty}\sum_{n=m}^{\infty}[\alpha_{mn}\mathbf{M}_{emn}^{r(4)}(k_0,\mathbf{r}) + \beta_{mn}\mathbf{N}_{omn}^{r(4)}(k_0,\mathbf{r})] \tag{9}$$

$$\mathbf{H}_s = \frac{j}{\eta_0}\sum_{m=0}^{\infty}\sum_{n=m}^{\infty}[\alpha_{mn}\mathbf{N}_{emn}^{r(4)}(k_0,\mathbf{r}) + \beta_{mn}\mathbf{M}_{omn}^{r(4)}(k_0,\mathbf{r})] \tag{10}$$

$$\mathbf{E}_t = \sum_{m=0}^{\infty}\sum_{n=m}^{\infty}[\gamma_{mn}\mathbf{M}_{emn}^{r(1)}(k_t,\mathbf{r}) + \delta_{mn}\mathbf{N}_{omn}^{r(1)}(k_t,\mathbf{r})] \tag{11}$$

$$\mathbf{H}_t = \frac{j}{\eta_t}\sum_{m=0}^{\infty}\sum_{n=m}^{\infty}[\gamma_{mn}\mathbf{N}_{emn}^{r(1)}(k_t,\mathbf{r}) + \delta_{mn}\mathbf{M}_{omn}^{r(1)}(k_t,\mathbf{r})] \tag{12}$$

with $k_t = \omega\sqrt{\mu_t\varepsilon_t}$ and $\eta_t = \sqrt{\mu_t/\varepsilon_t}$ being the wavenumber and wave impedance of the medium inside the spheroid.

The expansions of $\mathbf{E}_i'$ and $\mathbf{H}_i'$ in terms of vector spherical wave functions can be obtained from those of $-\mathbf{E}_i$ and $-\mathbf{H}_i$, respectively, by replacing θ_i by $\pi-\theta_i$. Thus, we have

$$\mathbf{E}_i' = \sum_{m=0}^{\infty}\sum_{n=m}^{\infty}[c_{mn}'\mathbf{M}_{emn}^{r(1)}(k_0,\mathbf{r}) + d_{mn}'\mathbf{N}_{omn}^{r(1)}(k_0,\mathbf{r})] \tag{13}$$

$$\mathbf{H}_i' = \frac{j}{\eta_0}\sum_{m=0}^{\infty}\sum_{n=m}^{\infty}[c_{mn}'\mathbf{N}_{emn}^{r(1)}(k_0,\mathbf{r}) + d_{mn}'\mathbf{M}_{omn}^{r(1)}(k_0,\mathbf{r})] \tag{14}$$

where $c_{mn}' = (-1)^{n-m}c_{mn}$ and $d_{mn}' = (-1)^{n-m+1}d_{mn}$.

The unknown scattered and transmitted electric and magnetic fields due to $\mathbf{E}_i'$ and $\mathbf{H}_i'$ can similarly be expanded in terms of vector spherical wave functions as

$$\mathbf{E}_s' = \sum_{m=0}^{\infty}\sum_{n=m}^{\infty}[\alpha_{mn}'\mathbf{M}_{emn}^{r(4)}(k_0,\mathbf{r}) + \beta_{mn}'\mathbf{N}_{omn}^{r(4)}(k_0,\mathbf{r})] \tag{15}$$

$$\mathbf{H}_s' = \frac{j}{\eta_0}\sum_{m=0}^{\infty}\sum_{n=m}^{\infty}[\alpha_{mn}'\mathbf{N}_{emn}^{r(4)}(k_0,\mathbf{r}) + \beta_{mn}'\mathbf{M}_{omn}^{r(4)}(k_0,\mathbf{r})] \tag{16}$$

$$\mathbf{E}_t' = \sum_{m=0}^{\infty}\sum_{n=m}^{\infty}[\gamma_{mn}'\mathbf{M}_{emn}^{r(1)}(k_t,\mathbf{r}) + \delta_{mn}'\mathbf{N}_{omn}^{r(1)}(k_t,\mathbf{r})] \quad (17)$$

$$\mathbf{H}_t' = \frac{j}{\eta_t}\sum_{m=0}^{\infty}\sum_{n=m}^{\infty}[\gamma_{mn}'\mathbf{N}_{emn}^{r(1)}(k_t,\mathbf{r}) + \delta_{mn}'\mathbf{M}_{omn}^{r(1)}(k_t,\mathbf{r})]. \quad (18)$$

EXPANDING THE FIELDS IN TERMS OF VECTOR WAVE FUNCTIONS (TM CASE)

For TM polarization, the electric field of the original incident wave can be written as

$$\mathbf{E}_i = (-\cos\theta_i\hat{\mathbf{x}} + \sin\theta_i\hat{\mathbf{z}})e^{-j\mathbf{k}_i\cdot\mathbf{r}} \quad (19)$$

and that of the image wave as

$$\mathbf{E}_i' = [-\cos(\pi-\theta_i)\hat{\mathbf{x}} + \sin(\pi-\theta_i)\hat{\mathbf{z}}]e^{-j\mathbf{k}_i'\cdot\mathbf{r}} \quad (20)$$

The electric and magnetic fields corresponding to the original incident wave can then be expanded in terms of vector spherical wave functions as

$$\mathbf{E}_i = -j\sum_{m=0}^{\infty}\sum_{n=m}^{\infty}[c_{mn}\mathbf{N}_{emn}^{r(1)}(k_0,\mathbf{r}) + d_{mn}\mathbf{M}_{omn}^{r(1)}(k_0,\mathbf{r})] \quad (21)$$

$$\mathbf{H}_i = \frac{1}{\eta_0}\sum_{m=0}^{\infty}\sum_{n=m}^{\infty}[c_{mn}\mathbf{M}_{emn}^{r(1)}(k_0,\mathbf{r}) + d_{mn}\mathbf{N}_{omn}^{r(1)}(k_0,\mathbf{r})] \quad (22)$$

and the unknown scattered and transmitted electromagnetic fields due to the original incident wave as

$$\mathbf{E}_s = -j\sum_{m=0}^{\infty}\sum_{n=m}^{\infty}[\tilde{\alpha}_{mn}\mathbf{N}_{emn}^{r(4)}(k_0,\mathbf{r}) + \tilde{\beta}_{mn}\mathbf{M}_{omn}^{r(4)}(k_0,\mathbf{r})] \quad (23)$$

$$\mathbf{H}_s = \frac{1}{\eta_0}\sum_{m=0}^{\infty}\sum_{n=m}^{\infty}[\tilde{\alpha}_{mn}\mathbf{M}_{emn}^{r(4)}(k_0,\mathbf{r}) + \tilde{\beta}_{mn}\mathbf{N}_{omn}^{r(4)}(k_0,\mathbf{r})] \quad (24)$$

$$\mathbf{E}_t = -j\sum_{m=0}^{\infty}\sum_{n=m}^{\infty}[\tilde{\gamma}_{mn}\mathbf{N}_{emn}^{r(1)}(k_t,\mathbf{r}) + \tilde{\delta}_{mn}\mathbf{M}_{omn}^{r(1)}(k_t,\mathbf{r})] \quad (25)$$

$$\mathbf{H}_t = \frac{1}{\eta_t}\sum_{m=0}^{\infty}\sum_{n=m}^{\infty}[\tilde{\gamma}_{mn}\mathbf{M}_{emn}^{r(1)}(k_t,\mathbf{r}) + \tilde{\delta}_{mn}\mathbf{N}_{omn}^{r(1)}(k_t,\mathbf{r})]. \quad (26)$$

The electric and magnetic fields corresponding to the image wave can now be expanded in terms of vector spherical wave functions as

$$\mathbf{E}_i' = -j\sum_{m=0}^{\infty}\sum_{n=m}^{\infty}[\tilde{c}_{mn}'\mathbf{N}_{emn}^{r(1)}(k_0,\mathbf{r}) + \tilde{d}_{mn}'\mathbf{M}_{omn}^{r(1)}(k_0,\mathbf{r})] \quad (27)$$

$$\mathbf{H}_i' = \frac{1}{\eta_0}\sum_{m=0}^{\infty}\sum_{n=m}^{\infty}[\tilde{c}_{mn}'\mathbf{M}_{emn}^{r(1)}(k_0,\mathbf{r}) + \tilde{d}_{mn}'\mathbf{N}_{omn}^{r(1)}(k_0,\mathbf{r})] \quad (28)$$

with $\tilde{c}_{mn}' = (-1)^{n-m+1}c_{mn}$, $\tilde{d}_{mn}' = (-1)^{n-m}d_{mn}$, and the unknown scattered and transmitted electromagnetic fields due to the image wave as

$$\mathbf{E}_s' = -j\sum_{m=0}^{\infty}\sum_{n=m}^{\infty}[\tilde{\alpha}_{mn}'\mathbf{N}_{emn}^{r(4)}(k_0,\mathbf{r}) + \tilde{\beta}_{mn}'\mathbf{M}_{omn}^{r(4)}(k_0,\mathbf{r})] \quad (29)$$

$$\mathbf{H}_s' = \frac{1}{\eta_0}\sum_{m=0}^{\infty}\sum_{n=m}^{\infty}[\tilde{\alpha}_{mn}'\mathbf{M}_{emn}^{r(4)}(k_0,\mathbf{r}) + \tilde{\beta}_{mn}'\mathbf{N}_{omn}^{r(4)}(k_0,\mathbf{r})] \quad (30)$$

$$\mathbf{E}_t' = -j\sum_{m=0}^{\infty}\sum_{n=m}^{\infty}[\tilde{\gamma}_{mn}'\mathbf{N}_{emn}^{r(1)}(k_t,\mathbf{r}) + \tilde{\delta}_{mn}'\mathbf{M}_{omn}^{r(1)}(k_t,\mathbf{r})] \quad (31)$$

$$\mathbf{H}_t' = \frac{1}{\eta_t}\sum_{m=0}^{\infty}\sum_{n=m}^{\infty}[\tilde{\gamma}_{mn}'\mathbf{M}_{emn}^{r(1)}(k_t,\mathbf{r}) + \tilde{\delta}_{mn}'\mathbf{N}_{omn}^{r(1)}(k_t,\mathbf{r})]. \quad (32)$$

BOUNDARY CONDITIONS

The boundary conditions require that the tangential components of the total electric and magnetic fields be continuous at the surface of the sphere. These can be expressed for the scattering due to the original incident wave as

$$[(\mathbf{E}_s + \mathbf{E}_i) \times \hat{\mathbf{r}}]\big|_{r=a} = [\mathbf{E}_t \times \hat{\mathbf{r}}]\big|_{r=a} \quad (33)$$

$$[(\mathbf{H}_s + \mathbf{H}_i) \times \hat{\mathbf{r}}]\big|_{r=a} = [\mathrm{H}_t \times \hat{\mathbf{r}}]\big|_{r=a} \quad (34)$$

and for the scattering due to the image wave as

$$[(\mathbf{E}_s' + \mathbf{E}_i') \times \hat{\mathbf{r}}]\big|_{r=a} = [\mathbf{E}_t' \times \hat{\mathbf{r}}]\big|_{r=a} \quad (35)$$

$$[(\mathbf{H}_s' + \mathbf{H}_i') \times \hat{\mathbf{r}}]\big|_{r=a} = [\mathbf{H}_t' \times \hat{\mathbf{r}}]\big|_{r=a} \quad (36)$$

where $\hat{\mathbf{r}}$ is the unit normal to the spherical surface. Substituting for the different electric and magnetic fields in (33)-(36) from (5)-(12) and (13)-(18) for TE polarization, and from (21)-(26) and (27)-(32) for TM polarization, integrating over the surface of the sphere, and using the orthogonal properties of the associated Legendre functions and the trigonometric functions, a set of linear equations can be obtained. These equations corresponding to TE polarization of the incident wave are given by

$$\gamma_{mn}\frac{j_n(k_t a)}{j_n(k_0 a)} - \alpha_{mn}\frac{h_n^{(2)}(k_0 a)}{j_n(k_0 a)} = c_{mn} \quad (37)$$

$$\gamma_{mn}\frac{[k_t a\, j_n(k_t a)]'}{[k_0 a\, j_n(k_0 a)]'}\frac{\mu_0}{\mu_t} - \alpha_{mn}\frac{[k_0 a\, h_n^{(2)}(k_0 a]'}{[k_0 a\, j_n(k_0 a)]'} = c_{mn} \quad (38)$$

$$\delta_{mn}\frac{[k_t a\, j_n(k_t a)]'}{[k_0 a\, j_n(k_0 a)]'}\frac{k_0}{k_t} - \beta_{mn}\frac{[k_0 a\, h_n^{(2)}(k_0 a]'}{[k_0 a\, j_n(k_0 a)]'} = d_{mn} \quad (39)$$

$$\delta_{mn}\frac{j_n(k_t a)}{j_n(k_0 a)}\frac{\eta_0}{\eta_t} - \beta_{mn}\frac{h_n^{(2)}(k_0 a)}{j_n(k_0 a)} = d_{mn} \quad (40)$$

$$\gamma_{mn}'\frac{j_n(k_t a)}{j_n(k_0 a)} - \alpha_{mn}'\frac{h_n^{(2)}(k_0 a)}{j_n(k_0 a)} = c_{mn}' \quad (41)$$

$$\gamma_{mn}'\frac{[k_t a\, j_n(k_t a)]'}{[k_0 a\, j_n(k_0 a)]'}\frac{\mu_0}{\mu_t} - \alpha_{mn}'\frac{[k_0 a\, h_n^{(2)}(k_0 a]'}{[k_0 a\, j_n(k_0 a)]'} = c_{mn}' \quad (42)$$

$$\delta_{mn}'\frac{[k_t a\, j_n(k_t a)]'}{[k_0 a\, j_n(k_0 a)]'}\frac{k_0}{k_t} - \beta_{mn}'\frac{[k_0 a\, h_n^{(2)}(k_0 a]'}{[k_0 a\, j_n(k_0 a)]'} = d_{mn}' \quad (43)$$

$$\delta_{mn}'\frac{j_n(k_t a)}{j_n(k_0 a)}\frac{\eta_0}{\eta_t} - \beta_{mn}'\frac{h_n^{(2)}(k_0 a)}{j_n(k_0 a)} = d_{mn}' \quad (44)$$

and those corresponding to the TM polarization of the incident wave are given by

$$\tilde{\gamma}_{mn}\frac{j_n(k_t a)}{j_n(k_0 a)}\frac{\eta_0}{\eta_t}-\tilde{\alpha}_{mn}\frac{h_n^{(2)}(k_0 a)}{j_n(k_0 a)}=c_{mn} \tag{45}$$

$$\tilde{\gamma}_{mn}\frac{[k_t a\, j_n(k_t a)]'}{[k_0 a\, j_n(k_0 a)]'}\frac{k_0}{k_t}-\tilde{\alpha}_{mn}\frac{[k_0 a\, h_n^{(2)}(k_0 a]'}{[k_0 a\, j_n(k_0 a)]'}=c_{mn} \tag{46}$$

$$\tilde{\delta}_{mn}\frac{[k_t a\, j_n(k_t a)]'}{[k_0 a\, j_n(k_0 a)]'}\frac{\mu_0}{\mu_t}-\tilde{\beta}_{mn}\frac{[k_0 a\, h_n^{(2)}(k_0 a]'}{[k_0 a\, j_n(k_0 a)]'}=d_{mn} \tag{47}$$

$$\tilde{\delta}_{mn}\frac{j_n(k_t a)}{j_n(k_0 a)}-\tilde{\beta}_{mn}\frac{h_n^{(2)}(k_0 a)}{j_n(k_0 a)}=d_{mn} \tag{48}$$

$$\tilde{\gamma}'_{mn}\frac{j_n(k_t a)}{j_n(k_0 a)}\frac{\eta_0}{\eta_t}-\tilde{\alpha}'_{mn}\frac{h_n^{(2)}(k_0 a)}{j_n(k_0 a)}=c'_{mn} \tag{49}$$

$$\tilde{\gamma}'_{mn}\frac{[k_t a\, j_n(k_t a)]'}{[k_0 a\, j_n(k_0 a)]'}\frac{k_0}{k_t}-\tilde{\alpha}'_{mn}\frac{[k_0 a\, h_n^{(2)}(k_0 a]'}{[k_0 a\, j_n(k_0 a)]'}=c'_{mn} \tag{50}$$

$$\tilde{\delta}'_{mn}\frac{[k_t a\, j_n(k_t a)]'}{[k_0 a\, j_n(k_0 a)]'}\frac{\mu_0}{\mu_t}-\tilde{\beta}'_{mn}\frac{[k_0 a\, h_n^{(2)}(k_0 a]'}{[k_0 a\, j_n(k_0 a)]'}=d'_{mn} \tag{51}$$

$$\tilde{\delta}'_{mn}\frac{j_n(k_t a)}{j_n(k_0 a)}-\tilde{\beta}'_{mn}\frac{h_n^{(2)}(k_0 a)}{j_n(k_0 a)}=d'_{mn} \tag{52}$$

with $j_n(ka)$, $h_n^{(2)}(ka)$ being the spherical Bessel function of the first kind and the spherical Hankel function of the second kind, respectively, of order *n* and argument *ka*.

The solution of these equations yields the unknown expansion coefficients, which can be expressed in matrix form for the case of TE polarization as

$$\begin{bmatrix}\alpha_{mn}\\ \beta_{mn}\\ \gamma_{mn}\\ \delta_{mn}\end{bmatrix}=\begin{bmatrix}s_n & 0\\ 0 & t_n\\ u_n & 0\\ 0 & v_n\end{bmatrix}\begin{bmatrix}c_{mn}\\ d_{mn}\end{bmatrix} \tag{53}$$

where

$$s_n=\frac{\mu_t j_n(q)[p\, j_n(p)]'-\mu_0 j_n(p)[q\, j_n(q)]'}{-\mu_t j_n(q)[p\, h_n^{(2)}(p)]'+\mu_0 h_n^{(2)}(p)[q\, j_n(q)]'} \tag{54}$$

$$t_n=\frac{-\varepsilon_t j_n(q)[p\, j_n(p)]'+\varepsilon_0 j_n(p)[q\, j_n(q)]'}{\varepsilon_t j_n(q)[p\, h_n^{(2)}(p)]'-\varepsilon_0 h_n^{(2)}(p)[q\, j_n(q)]'} \tag{55}$$

$$u_n=\frac{jp^{-1}}{-\mu_t j_n(q)[p\, h_n^{(2)}(p)]'+\mu_0 h_n^{(2)}(p)[q\, j_n(q)]'} \tag{56}$$

$$v_n=\frac{-jqp^{-2}}{\varepsilon_t j_n(q)[p\, h_n^{(2)}(p)]'-\varepsilon_0 h_n^{(2)}(p)[q\, j_n(q)]'} \tag{57}$$

and

$$\begin{bmatrix}\alpha'_{mn}\\ \beta'_{mn}\\ \gamma'_{mn}\\ \delta'_{mn}\end{bmatrix}=\begin{bmatrix}s_n & 0\\ 0 & t_n\\ u_n & 0\\ 0 & v_n\end{bmatrix}\begin{bmatrix}c'_{mn}\\ d'_{mn}\end{bmatrix} \tag{58}$$

in which $q=k_t a$ and $p=k_0 a$. The solution for the case of TM polarization can be expressed in matrix form as

$$\begin{bmatrix}\tilde{\alpha}_{mn}\\ \tilde{\beta}_{mn}\\ \tilde{\gamma}_{mn}\\ \tilde{\delta}_{mn}\end{bmatrix}=\begin{bmatrix}t_n & 0\\ 0 & s_n\\ v_n & 0\\ 0 & u_n\end{bmatrix}\begin{bmatrix}c_{mn}\\ d_{mn}\end{bmatrix} \tag{59}$$

and

$$\begin{bmatrix}\tilde{\alpha}'_{mn}\\ \tilde{\beta}'_{mn}\\ \tilde{\gamma}'_{mn}\\ \tilde{\delta}'_{mn}\end{bmatrix}=\begin{bmatrix}t_n & 0\\ 0 & s_n\\ v_n & 0\\ 0 & u_n\end{bmatrix}\begin{bmatrix}c'_{mn}\\ d'_{mn}\end{bmatrix}. \tag{60}$$

FAR FIELD

The scattered electric field in the far zone is obtained by considering the asymptotic forms of the vector spherical wave functions, which are dependent on the asymptotic forms of the spherical Hankel function and its derivative. These asymptotic forms can be written as [13, 14]

$$\lim_{r\to\infty}[h_n^{(2)}(kr)]\to j^{n+1}\frac{e^{-jkr}}{kr}$$

$$\lim_{r\to\infty}\left\{\frac{1}{kr}\frac{\partial}{\partial kr}[krh_n^{(2)}(kr)]\right\}\to j^n\frac{e^{-jkr}}{kr}.$$

Thus, the scattered electric field in the far zone can be written as $\mathbf{E}_s(r,\theta,\phi)+\mathbf{E}'_s(r,\theta,\phi)$, where

$$\mathbf{E}_s(r,\theta,\phi)=\frac{e^{-jkr}}{kr}\sum_{m=0}^{\infty}\sum_{n=m}^{\infty}[F_{s\theta}(\theta,\phi)\hat{\theta}+F_{s\phi}(\theta,\phi)\hat{\phi}] \tag{61}$$

in which

$$F_{s\theta}(\theta,\phi)=j^n[-\frac{jmP_n^m(\cos\theta)}{\sin\theta}\alpha_{mn}+\frac{\partial P_n^m(\cos\theta)}{\partial\theta}\beta_{mn}]\times\sin(m\phi) \tag{62}$$

$$F_{s\phi}(\theta,\phi)=j^n[-j\frac{\partial P_n^m(\cos\theta)}{\partial\theta}\alpha_{mn}+\frac{mP_n^m(\cos\theta)}{\sin\theta}\beta_{mn}]\times\cos(m\phi) \tag{63}$$

in the case of TE polarization, and

$$F_{s\theta}(\theta,\phi)=j^n[-j\frac{\partial P_n^m(\cos\theta)}{\partial\theta}\tilde{\alpha}_{mn}+\frac{mP_n^m(\cos\theta)}{\sin\theta}\tilde{\beta}_{mn}]\times\cos(m\phi) \tag{64}$$

$$F_{s\phi}(\theta,\phi)=j^n[-\frac{jmP_n^m(\cos\theta)}{\sin\theta}\tilde{\alpha}_{mn}+\frac{\partial P_n^m(\cos\theta)}{\partial\theta}\tilde{\beta}_{mn}]\times\sin(m\phi) \tag{65}$$

in the case of TM polarization, and

$$\mathbf{E}'_s(r,\theta,\phi)=\frac{e^{-jkr}}{kr}\sum_{m=0}^{\infty}\sum_{n=m}^{\infty}[F'_{s\theta}(\theta,\phi)\hat{\theta}+F'_{s\phi}(\theta,\phi)\hat{\phi}]. \tag{66}$$

Explicit expressions of functions $F'_{s\theta}(\theta,\phi)$ and $F'_{s\phi}(\theta,\phi)$ can be obtained from the corresponding expressions of $F_{s\theta}(\theta,\phi)$ and $F_{s\phi}(\theta,\phi)$, respectively, by replacing the coefficients $\alpha_{mn}, \beta_{mn}, \tilde{\alpha}_{mn}$, and $\tilde{\beta}_{mn}$ by $\alpha'_{mn}, \beta'_{mn}, \tilde{\alpha}'_{mn}$, and $\tilde{\beta}'_{mn}$, respectively.

The magnitude of the scattering cross section $\sigma(\theta,\phi)$ is given by

$$\sigma(\theta,\phi) = \lim_{r\to\infty} 4\pi r^2 \frac{\left|\mathbf{E}_s(r,\theta,\phi) + \mathbf{E}'_s(r,\theta,\phi)\right|^2}{\left|\mathbf{E}_i(r,\theta,\phi)\right|^2} \tag{67}$$

where $\left|\mathbf{E}_i(r,\theta,\phi)\right|$ is the magnitude of the incident wave, which is unity in this case. After substituting from (61) and (66) in (67), we can write the magnitude of the normalized scattering cross section as

$$\frac{\pi\sigma(\theta,\phi)}{\lambda^2} = \left|F''_{s\theta}(\theta,\phi)\right|^2 + \left|F''_{s\phi}(\theta,\phi)\right|^2 \tag{68}$$

where $F''_{s\psi} = F_{s\psi}(\theta,\phi) + F'_{s\psi}(\theta,\phi)$ for $\psi = \theta,\phi$.

The normalized backscattering cross section is obtained from (68) for $\theta = \theta_i$ and $\phi = 0$:

$$\frac{\pi\sigma(\theta_i)}{\lambda^2} = \left|F''_{s\theta}(\theta_i,0)\right|^2 + \left|F''_{s\phi}(\theta_i,0)\right|^2. \tag{69}$$

NUMERICAL RESULTS

Results are presented as normalized backscattering cross sections for spheres of different sizes made of DPS, DNG, ENG, and MNG materials. Since the expressions for the various electromagnetic fields and the normalized backscattering cross section are in the form of infinite series, to obtain numerical results, these series have to be truncated appropriately. From the numerical experiments performed, we have found that for all the results that we have obtained, it is sufficient to consider the index *m* in the series from 0 to (*ka*+4), with *ka* being the radius of the sphere *a* multiplied by the wavenumber, and the index *n* to be from *m* to *m*+8, to get a two significant digit accuracy.

To verify our analysis and the accuracy of the results obtained, we have calculated the normalized backscattering cross sections for a sphere of size *ka*=0.1 for both TE and TM polarizations of the incident wave, and compared these results with those obtained from [1]. The expressions of the backscattering cross-section magnitudes as obtained from [1] are

$$\frac{\pi\sigma(\theta_i)}{\lambda^2} = 20\log_{10}(0.001\cos^2\theta_i)\ \text{dB}$$

for TE polarization, and

$$\frac{\pi\sigma(\theta_i)}{\lambda^2} = 20\log_{10}[0.001(2\sin^2\theta_i + 1)]\ \text{dB}$$

for TM polarization.

These magnitudes are plotted in Fig. (**3**), together with the corresponding magnitudes of the backscattering cross section calculated using our analysis, by substituting $\varepsilon_r = \varepsilon_t/\varepsilon_0 = 10^{18}$, $\mu_r = \mu_t/\mu_0 = 10^{-18}$. The results are in very good agreement, verifying our analysis and the accuracy of the results.

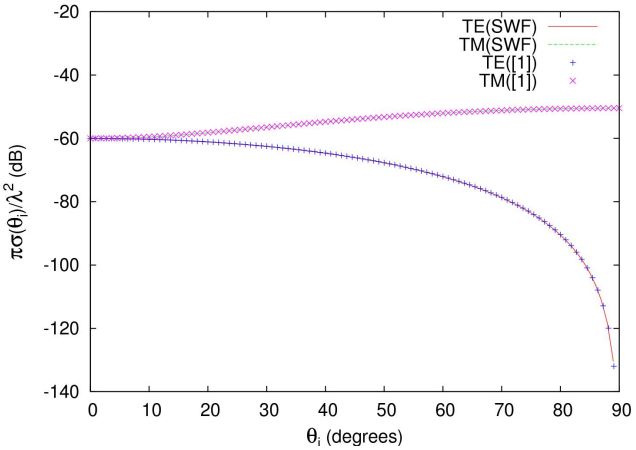

Fig. (3). Normalized backscattering cross section magnitudes obtained from our analysis (SWF) and from [1].

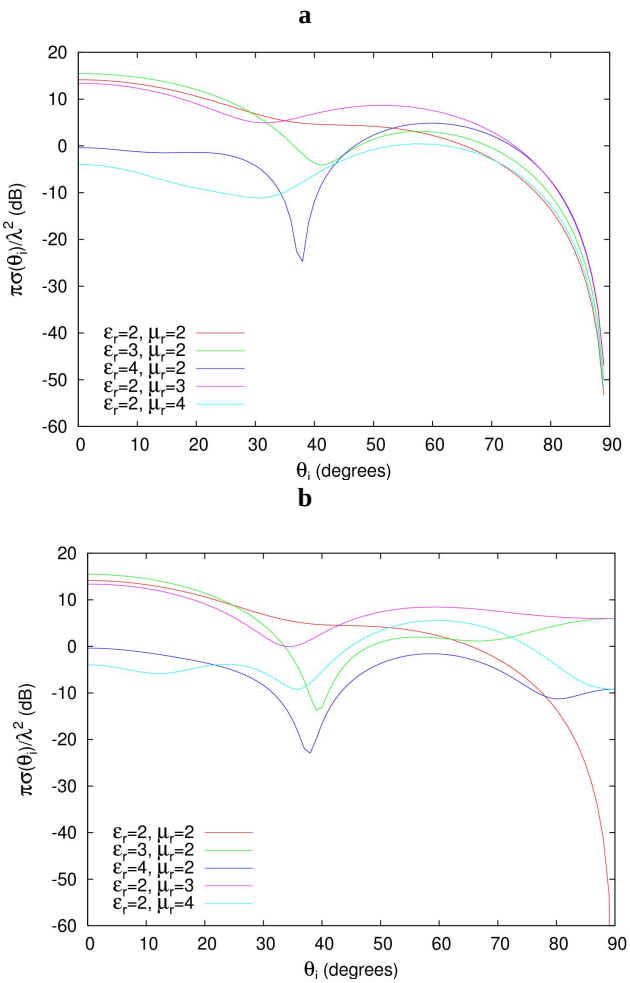

Fig. (4). Variations of normalized backscattering cross section magnitudes with the angle of incidence, for spherical bosses made of different DPS metamaterials, for (**a**) TE and (**b**) TM polarization of the incident wave.

Fig. (**4**) shows the variations of the normalized backscattering cross section magnitudes with the incident angle for spherical bosses of radius *ka*=2 made of DPS materials of relative permittivity (ε_r) 2.0, 3.0, 4.0, and relative permeability (μ_r) 2.0, 3.0, 4.0, for both TE and TM polarizations of the incident wave. As ε_r increases with μ_r remaining constant at 2.0, we find a sharpening of the minima, for both polarizations. On the other hand, when μ_r increases with ε_r remaining constant at 2.0, the sharpening of the minima is much less. When the angle of incidence is larger than about 60 degrees, the magnitudes of the scattering cross sections for TE polarization steadily decreases for all ε_r and μ_r combinations. But for TM polarization, this happens only when $\varepsilon_r = \mu_r = 2$.

Variations of normalized backscattering cross section magnitudes with the incident angle for spherical bosses of radius *ka*=2 made of DNG materials are shown in Fig. (**5**), for both TE and TM polarizations of the incident wave. Since both ε_r and μ_r are negative for a DNG metamaterial, the wavenumber becomes negative within the metamaterial medium, but the wave impedance remains positive.

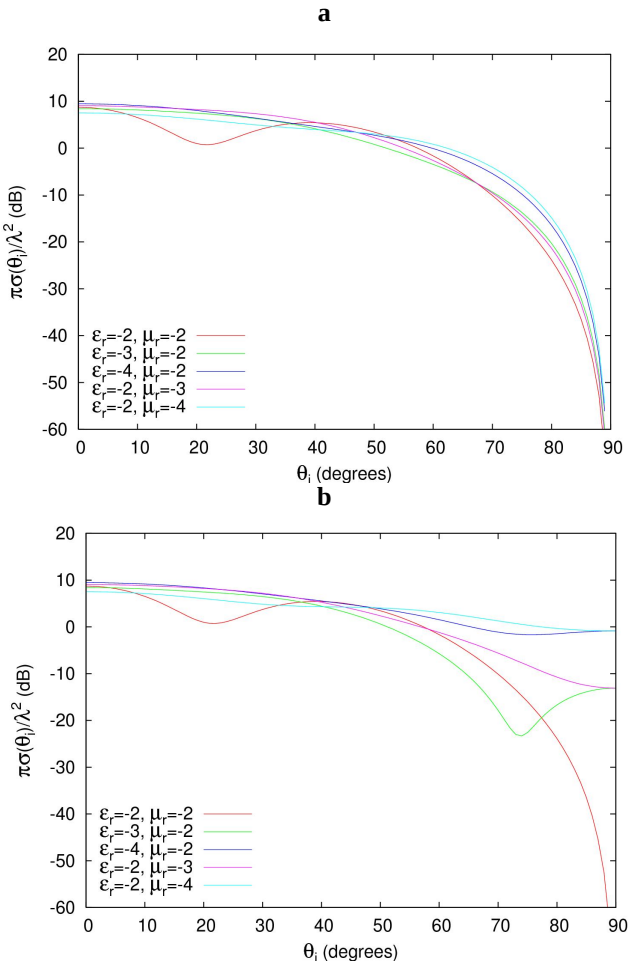

Fig. (5). Variations of normalized backscattering cross section magnitudes with the angle of incidence for spherical bosses made of different DNG metamaterials, for (**a**) TE and (**b**) TM polarization of the incident wave.

In this case, for TE polarization of the incident wave, the magnitudes of all the scattering cross sections steadily decrease as the angle of incidence increases from 0 to 90 degrees, except for that corresponding to relative permittivity 2.0 and relative permeability 2.0. When considering the case corresponding to TM polarization, we find that the scattering cross section magnitudes for ε_r=-3.0, μ_r=-2.0 and ε_r=-2.0, μ_r=-3.0 are higher than those for ε_r=-4.0, μ_r=-2.0 and ε_r=-2.0, μ_r=-4.0 at 90 degree angle of incidence, in contrast to the opposite in Fig. (**4b**) for a DPS metamaterial. Also, the magnitudes of the different scattering cross sections at 0 degrees are almost the same in contrast to those in Fig. (**4**).

Fig. (**6**) shows the variations of the normalized backscattering cross section magnitudes with the angle of incidence for spherical bosses of radius *ka*=2 made of ENG metamaterials, for both TE and TM polarizations of the incident wave. In this case, since ε_r is negative and μ_r is positive, the wavenumber and the wave impedance are both negative imaginary numbers.

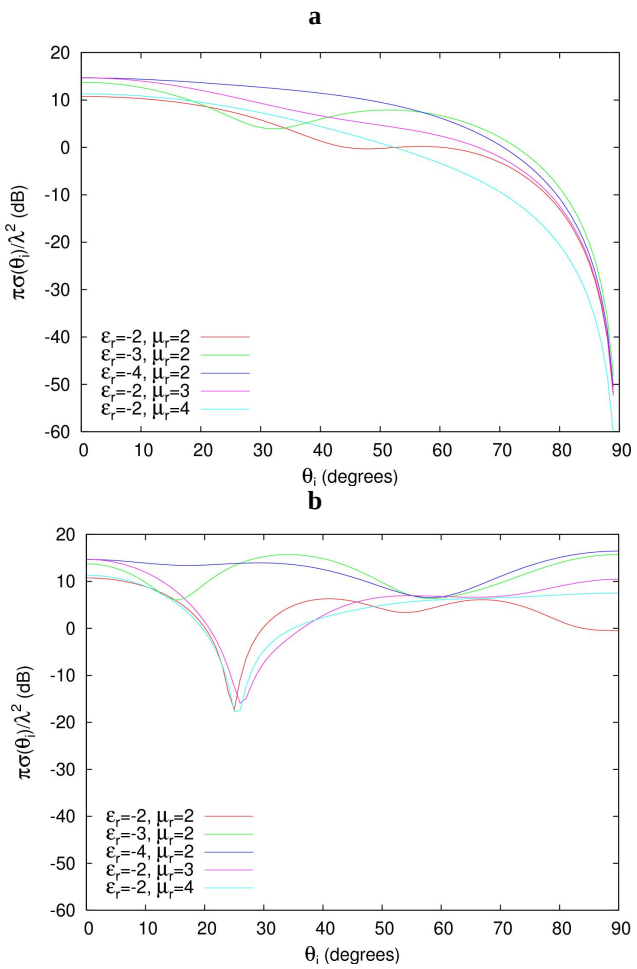

Fig. (6). Variations of normalized backscattering cross section magnitudes with the angle of incidence for bosses made of different ENG metamaterials, for (**a**) TE and (**b**) TM polarization of the incident wave.

Again for the TE polarization of the incident wave, we can observe the magnitudes of the scattering cross sections decreasing steadily with the angle of incidence, except for the cases ε_r=-2.0, μ_r=2.0 and ε_r=-3.0, μ_r=2.0.

For TM polarization of the incident wave, scattering cross section magnitudes are more oscillatory with much

sharper minima and are higher in value when the angle of incidence is 90 degrees, than for the cases corresponding to DPS and DNG metamaterials.

Variations of normalized backscattering cross section magnitudes with the incident angle for spherical bosses of radius *ka*=2 made of MNG metamaterials are shown in Fig. (**7**) for both TE and TM polarizations of the incident wave. In this case, since ε_r is positive and μ_r is negative, the wave-number is negative imaginary, but the wave impedance is positive imaginary.

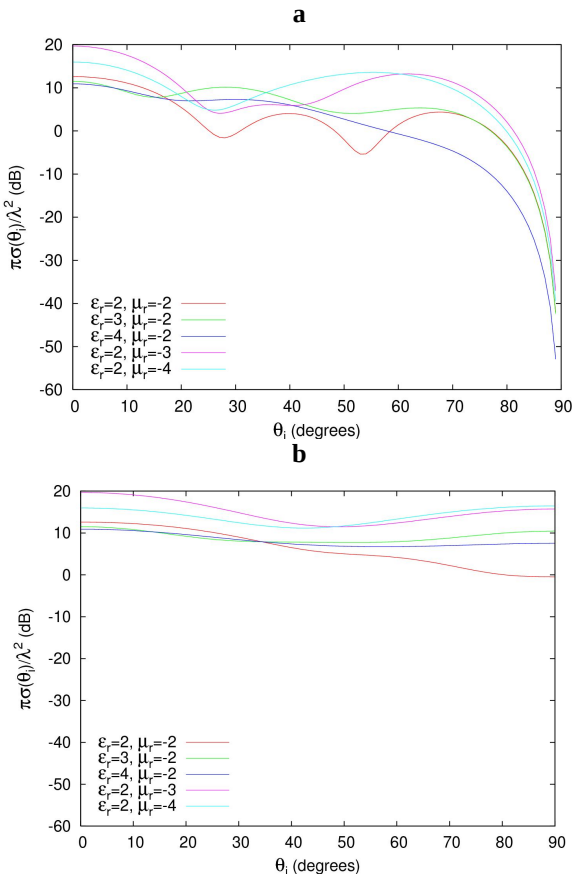

Fig. (7). Variations of normalized backscattering cross section magnitudes with the angle of incidence for bosses made of different MNG metamaterials, for (**a**) TE and (**b**) TM polarization of the incident wave.

In Fig. (**7a**), the magnitudes of the scattering cross sections are oscillatory for lower values of ε_r and μ_r. However, as the values of ε_r and μ_r increase, the oscillatory behavior becomes reduced. In Fig. (**7b**), the variations in magnitudes of the scattering cross sections with the angle of incidence become less significant as ε_r and μ_r increase. In this case, the magnitudes of the cross sections also remain at a relatively higher value.

Fig. (**8**) shows the variations of the normalized back-scattering cross section magnitudes with the angle of incidence for spherical bosses of different radii, made of a DPS material with ε_r=3.0 and μ_r=2.0, for both TE and TM polarization of the incident wave. When referring to these figures, we find that the scattering cross section magnitudes in general become higher for both polarizations as the size of the sphere increases. This is due to the area available for scattering becoming larger for a bigger sphere. Also, for TM polarization, we can observe an increase in the oscillatory nature of the patterns with the size of the sphere.

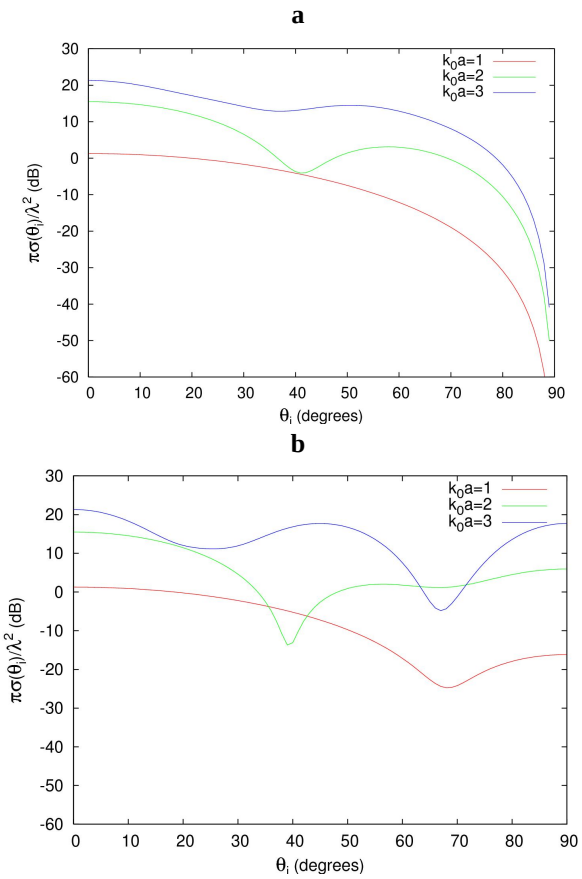

Fig. (8). Variations of normalized backscattering cross section magnitudes with the angle of incidence for DPS bosses of different radii with ε_r=3.0, μ_r=2.0, for (**a**) TE and (**b**) TM polarization of the incident wave.

Fig. (**9**) shows the variations of the normalized back-scattering cross section magnitudes with the angle of incidence for spherical bosses of the same size as those considered in Fig. (**8**), but made up of a MNG metamaterial with ε_r=3.0 and μ_r=-2.0, for both TE and TM polarizations of the incident wave.

When compared to Fig. (**8**), we find that the cross sections in this case are more oscillatory for TE polarization, but less oscillatory for TM polarization. However, as the size of the sphere increases, the oscillatory behavior of the curves increases for both TE and TM polarizations.

CONCLUSION

An exact solution has been presented to the problem of scattering of a plane wave from a metamaterial boss on an infinite conducting plane, using the method of separation of variables. Numerical results have been presented as normalized backscattering cross sections for bosses of different sizes made up of DPS, DNG, ENG, and MNG metamaterials, to show the effects of these on the scattering cross sections.

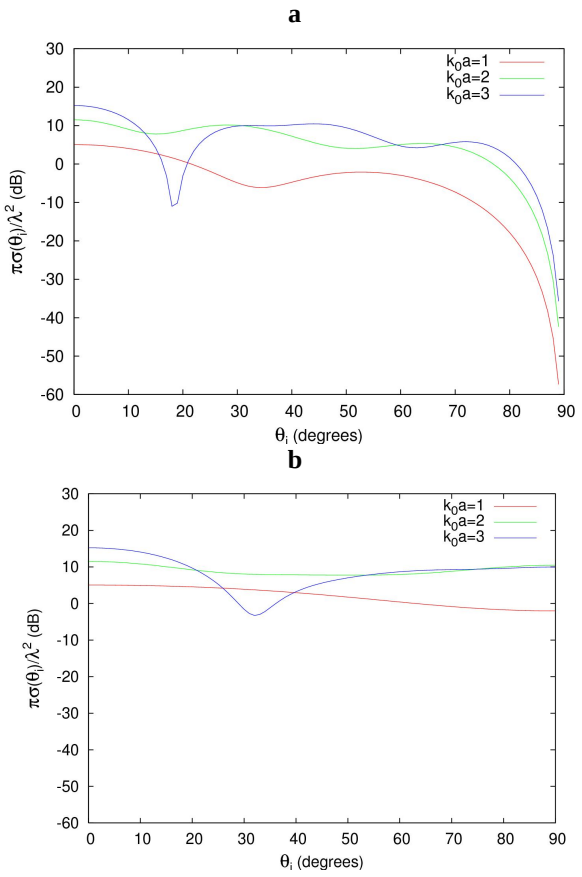

Fig. (9). Variations of normalized backscattering cross section magnitudes with the angle of incidence for MNG bosses of different radii with ε_r=3.0 and μ_r=-2.0, for (**a**) TE and (**b**) TM polarization of the incident wave.

APPENDIX

The vector spherical wave functions **M** and **N** used in the analysis are defined in terms of the spherical scalar wave function

$$\psi^{(i)}_{\substack{e\\o}mn}(r,\theta,\phi) = z_n^{(i)}(kr)P_n^m(\cos\theta)\begin{matrix}\cos\\\sin\end{matrix} m\phi \tag{70}$$

where $z_n^{(i)}(kr)$ is the spherical Bessel function of order *n*, kind *i*, and argument *kr* with *k* being the wave-number of the medium, and $P_n^m(\cos\theta)$ is the associated Legendre function of order m, degree n, and argument cos θ.

$$\mathbf{M}^{r(i)}_{\substack{e\\o}mn}(r,\theta,\phi) = \nabla\psi^{(i)}_{\substack{e\\o}mn}(r,\theta,\phi)\times\hat{\mathbf{r}} \tag{71}$$

where $\hat{\mathbf{r}}$ is the unit position vector, and

$$\mathbf{N}^{r(i)}_{\substack{e\\o}mn}(r,\theta,\phi) = k^{-1}[\nabla\times\mathbf{M}^{r(i)}_{\substack{e\\o}mn}(r,\theta,\phi)]. \tag{72}$$

REFERENCES

[1] V. Twersky, "On the nonspecular reflection of electromagnetic waves", *J. App. Phys*., vol. 22, pp. 825-835, 1951.

[2] A.-K. Hamid, I.R. Ciric, and M. Hamid, "Electromagnetic scattering by hemispherical bosses on an infinite plane surface", in Proceedings, IEEE Antennas and Propagation Society International Symposium, 1993, pp. 82-85.

[3] A.-K. Hamid and M. Hussein, "Iterative solution to the scattering by hemispherical bosses on a conducting surface", in Proceedings, IEEE Antennas and Propagation Society International Symposium, 1994, pp. 225-228.

[4] A.-K. Hamid, "Multiple scattering of a plane electromagnetic wave by hemispherical bosses on an infinite plane", *Can. J. Phys*., vol. 74, pp. 108-113, 1996.

[5] I.R. Ciric and F.R. Cooray, "Scattering of a plane wave by a hemispheroidal boss on an infinite plane", *Can. J. Phys*., vol. 70, pp. 615-622, 1992.

[6] H. Sakurai, M. Ohki, K. Motojima, and S. Kozaki, "Scattering of Gaussian beam from a hemispherical boss on a conducting plane", *IEEE Trans. Antennas Propag.*, vol. 52, pp. 892-894, March 2004.

[7] R.W. Ziolkowski and N. Engheta, "Metamaterial special issue introduction", *IEEE Trans. Antennas Propag.*, vol. 51, pp. 2546-2549, October 2003.

[8] A. Alu and N. Engheta, "Peculiar radar cross-section properties of double-negative and single-negative metamaterials", in Proceedings, IEEE Radar Conference, 2004, pp. 91-93.

[9] A. Alu, N. Engheta, A. Erentok, and R.W. Ziolkowski, "Single-negative, double-negative, and low-index meta-materials and their electromagnetic applications", *IEEE Antennas Propag. Mag.*, vol. 49, pp. 23-36, February 2007.

[10] N. Engheta and R.W. Ziolkowski, "A positive future for double-negative metamaterials", *IEEE Trans. Microw. Theory Tech.*, vol. 53, pp. 1535-1556, April 2005.

[11] J.A. Stratton, *Electromagnetic Theory*. New York: Mc-Graw Hill, 1941.

[12] D.S. Jones, *The Theory of Electromagnetism*. New York: Pergamon Press, 1964.

[13] R.F. Harrington, *Time Harmonic Electromagnetic Fields*. New York: Mc-Graw Hill, 1961.

[14] N.W. McLachlan, *Bessel Functions for Engineers*. London: Oxford University Press, 1955.

Received: March 03, 2008 Revised: July 04, 2008 Accepted: August 15, 2008